

Polarized radiation from a point source orbiting a Schwarzschild black hole

Serge Pineault *Institute of Astronomy, Madingley Road, Cambridge CB3 0HA*

Received 1976 November 10

Summary. The effects of a strong gravitational field on the polarized radiation coming from a point source orbiting a Schwarzschild black hole are investigated. It is shown that, for a source with intrinsic polarization properties, although no rotation of the polarization plane occurs along a given ray, the observed position angle of the polarization vector changes significantly during the orbital period.

1 Introduction

The study of the polarization properties associated with the radiation coming from a source orbiting a black hole is of considerable interest. In most cases, where the wavelength of the radiation is much smaller than the other scales present, it is sufficient to use the laws of geometrical optics in curved spacetime, according to which the polarization vector is perpendicular to the rays and parallelly propagated along them. This approach was recently applied to the case of a source orbiting a Kerr black hole, in an attempt to obtain the angle through which the polarization plane rotates along a given ray (Pineault 1975; Pineault & Roeder 1977a, b), thus giving a direct indication of the effect of frame dragging on the polarization plane.

However, an observationally more significant quantity is the periodic variation of the position angle of the radiation coming from a source of constant intrinsic polarization properties in orbit around a black hole. This is totally different and must not be confused with the rotation of the polarization plane along a given ray. In contrast, the relevant quantity, here, is the relative position angle of the radiation coming along different rays (source at different positions on its orbit), assuming that the polarization properties of the source remain constant (e.g. polarization vector always parallel to an intrinsic symmetry axis). In fact, such a periodic variation of the position angle is present even in a spherically symmetric field, where no rotation occurs along any given ray. This is purely due to a combination of the general relativistic light deflection and special relativistic aberration. Pulsars (or pulsar-like objects) and accretion disks with specific polarization properties (Rees 1975) are examples of the type of sources to which this analysis can be applied.

In what follows, we shall then consider a restricted but illustrative case in which a discrete source of radiation is in orbit around a Schwarzschild black hole at a constant radius and

constant circular velocity, and where perturbing effects (such as gravitational radiation etc) are negligible. We use units where $G = c = 1$.

2 General outline

The black hole is at the origin of a spherical coordinate system and the observer is at rest at a large distance ($r_0 \rightarrow \infty$) and at some polar angle θ_0 . The source of radiation moves on a direct circular orbit in the equatorial plane at a distance r_s . The observed position angle (PA) is then defined as the angle measured relative to the projected z axis.

Before proceeding further, we note that:

(a) in any given gravitational field, the angle between two polarization directions is constant along any given ray, and

(b) in a Schwarzschild field, the polarization vector, as measured by static observers, keeps a fixed orientation with respect to the angular momentum vector \mathbf{l} of the ray trajectory (the vector \mathbf{l} being defined as the normal to the plane of the trajectory). This last property follows from symmetry considerations or can be obtained by direct calculation (Pineault 1975) and it is only true in a field with spherical symmetry since only then does any ray trajectory lie in a plane.

For each ray connecting the source to the observer, the observed PA is then obtained as follows. The polarization vector, in the source's local rest frame (SLRF), is assumed known. Because of property (a) above, we can arbitrarily choose it parallel to the z axis, *as measured in the SLRF*. We then make a transformation to a local static frame (LSF) at the same position as the source. In this LSF, we evaluate the angle ψ between the polarization vector and the angular momentum vector of the ray trajectory which, because of property (b), is also the same angle as observed in the observer's rest frame at infinity. From this angle and the observed position of the image with respect to the position of the black hole on the celestial sphere, we obtain the position angle by simple trigonometry.

3 Mathematical formulation

The metric has the usual form

$$ds^2 = -(1 - 2m/r) dt^2 + (1 - 2m/r)^{-1} dr^2 + r^2(d\theta^2 + \sin^2 \theta d\phi^2). \quad (1)$$

The local static frame (LSF) is the one for which the basic one-forms are

$$\begin{aligned} \omega^{(t)} &= (1 - 2m/r)^{1/2} dt, & \omega^{(r)} &= (1 - 2m/r)^{-1/2} dr, \\ \omega^{(\theta)} &= r d\theta, & \omega^{(\phi)} &= r \sin \theta d\phi. \end{aligned} \quad (2)$$

If the source (SLRF) moves with velocity v in the $+\phi$ direction with respect to the LSF, then its basis one-forms are simply

$$\omega^{\hat{a}} = L^{\hat{a}}_{(b)} \omega^{(b)},$$

where

$$L^{\hat{a}}_{(b)} = \begin{bmatrix} \gamma & 0 & 0 & \gamma v \\ 0 & 1 & 0 & 0 \\ 0 & 0 & 1 & 0 \\ \gamma v & 0 & 0 & 1 \end{bmatrix}, \quad (3)$$

$$\gamma = (1 - v^2)^{-1/2}.$$

We systematically use brackets and hats to denote LSF and SLRF indices respectively. Both frames are local orthonormal frames in the sense that the basis vectors satisfy $\mathbf{e}_{\hat{a}} \cdot \mathbf{e}_{\hat{b}} = \eta_{\hat{a}\hat{b}}$, $\mathbf{e}_{(a)} \cdot \mathbf{e}_{(b)} = \eta_{(a)(b)}$, where η is the Minkowski metric: $\eta = \text{Diag}(-1, 1, 1, 1)$.

The ray vector $k^\alpha = dx^\alpha/d\tau$, with τ an affine parameter, is the solution of the null geodesic equations of the metric (1). The general LSF components are, with a convenient normalization

$$k^{(t)} = \frac{1}{(1 - 2m/r)^{1/2}}, \quad k^{(r)} = \pm \frac{[r^4 - r^2(1 - 2m/r)(l^2 + q)]^{1/2}}{r^2(1 - 2m/r)^{1/2}}, \quad (4)$$

$$k^{(\theta)} = \pm \frac{[q - l^2 \cot^2 \theta]^{1/2}}{r}, \quad k^{(\phi)} = \frac{l}{r},$$

where the parameters l and q are constants of the motion and the circular velocity is $v_{\text{cir}} = (m/(r - 2m))^{1/2}$ (see Bardeen, Press & Teukolsky 1972, with their parameter $a = 0$).

We now express the needed quantities in terms of $k^{(a)}$ and $\hat{k}^{\hat{a}}$. Let $f^{\hat{a}}$ be the polarization vector parallel to the projected symmetry axis ($\pm \mathbf{e}_{\hat{\theta}}$ direction), i.e. $f^{\hat{a}} \propto \mathbf{e}_{\hat{\theta}} + K \hat{k}^{\hat{a}}$, with $K = \text{constant}$. By requiring $f^{\hat{a}} \hat{f}_{\hat{a}} = 1$, $f^{\hat{a}} \hat{k}_{\hat{a}} = 0$, we find

$$f^{\hat{a}} = \frac{1}{k^{\hat{t}}(k^{\hat{t}^2} - k^{\hat{\theta}^2})^{1/2}} (0, -k^{\hat{\theta}} k^{\hat{r}}, k^{\hat{t}^2} - k^{\hat{\theta}^2}, -k^{\hat{\theta}} k^{\hat{\phi}}). \quad (5)$$

Transforming this vector to the LSF, it follows

$$f^{(a)} = \frac{1}{k^{\hat{t}}(k^{\hat{t}^2} - k^{\hat{\theta}^2})^{1/2}} (-\gamma v k^{\hat{\theta}} k^{\hat{\phi}}, -k^{\hat{\theta}} k^{\hat{r}}, k^{\hat{t}^2} - k^{\hat{\theta}^2}, -\gamma k^{\hat{\theta}} k^{\hat{\phi}}). \quad (6)$$

One can eliminate the time component of $f^{(a)}$ by transforming to $p^{(a)} = f^{(a)} + \alpha k^{(a)}$, $\alpha = \text{constant}$, without affecting any of the physical measurements. However, this is not necessary as will be seen later. The angular momentum vector of the ray trajectory, defined in the LSF, is

$$l^{(a)} = (0, 0, -k^{(\phi)}, k^{(\theta)}) / (k^{(\phi)^2} + k^{(\theta)^2})^{1/2}. \quad (7)$$

Both $p^{(a)}$ and $l^{(a)}$ are purely spacelike unit vectors and normal to $k^{(a)}$, so we can write $p^{(a)} = (0, \mathbf{p}) = (f^{(t)} + \alpha k^{(t)}, \mathbf{f} + \alpha \mathbf{k})$, $l^{(a)} = (0, \mathbf{l})$, and the angle ψ between them satisfies

$$\cos \psi = \mathbf{l} \cdot \mathbf{p} = \mathbf{l} \cdot \mathbf{f},$$

$$\sin \psi = (\mathbf{l} \times \mathbf{p}) \cdot \frac{\mathbf{k}}{|\mathbf{k}|} = (\mathbf{l} \times \mathbf{f}) \cdot \frac{\mathbf{k}}{k^{(t)}}, \quad (8)$$

where a bold type denotes a 3-vector in the LSF and we have used the fact that

$$\mathbf{k} \cdot \mathbf{l} = k^{(a)} l_{(a)} = 0 = k^{(a)} k_{(a)} = k^{(t)^2} - |\mathbf{k}|^2.$$

The angle ψ is measured counterclockwise from \mathbf{l} to \mathbf{p} as seen by an observer looking at the incident radiation.

Straightforward calculations yield

$$\cos \psi = -[k^{(\phi)}(k^{\hat{t}^2} - k^{(\theta)^2}) + \gamma k^{(\theta)^2} k^{\hat{\phi}}] / X, \quad (9)$$

$$\sin \psi = -k^{\hat{t}} k^{(\theta)} k^{(r)} (k^{\hat{t}} + \gamma v k^{(\phi)}) / X k^{(t)},$$

where

$$X = k^{\hat{t}}(k^{\hat{t}^2} - k^{(\theta)^2})^{1/2} (k^{(\theta)^2} + k^{(\phi)^2})^{1/2},$$

and we have used the fact that $k^{\hat{\theta}} = k^{(\theta)}$, $k^{\hat{r}} = k^{(r)}$.

The next step consists in obtaining the polarization angle PA in terms of ψ and the position of the image with respect to the black hole. Following Cunningham & Bardeen (1973), we let α and β be the apparent displacement of the image perpendicular to and parallel to the projected z axis. Then $\alpha = -l/\sin \theta_0$, $\beta = (q - l^2 \cot^2 \theta_0)^{1/2}$, and $\mathbf{l} = (\beta \mathbf{e}_{(\alpha)} - \alpha \mathbf{e}_{(\beta)})/(\alpha^2 + \beta^2)^{1/2}$, where $\mathbf{e}_{(\alpha)}$ and $\mathbf{e}_{(\beta)}$ are unit vectors corresponding to the (Cartesian) coordinates α and β . The projected z axis is along $\mathbf{e}_{(\beta)}$ and, by simple trigonometry, we find

$$\cos(\text{PA}) = (-\alpha \cos \psi + \beta \sin \psi)/(\alpha^2 + \beta^2)^{1/2}, \quad (10)$$

$$\sin(\text{PA}) = -(\beta \cos \psi + \alpha \sin \psi)/(\alpha^2 + \beta^2)^{1/2}.$$

Another interesting physical quantity is the direction of emission at the source as seen in the SLRF. It is specified by the angles ω and χ where ω is an azimuthal angle in the equatorial plane, measured counter-clockwise from the local outward radial direction $+\mathbf{e}_r$ and χ is a polar angle measured from the z axis $-\mathbf{e}_\theta$. They are given by

$$\begin{aligned} \sin \omega &= k^{\hat{r}}/(k^{\hat{r}^2} + k^{\hat{\phi}^2})^{1/2}, \\ \cos \omega &= k^{\hat{\phi}}/(k^{\hat{r}^2} + k^{\hat{\phi}^2})^{1/2}, \\ \cos \chi &= -k^{\hat{\theta}}/k^{\hat{t}}, \end{aligned} \quad (11)$$

and

$$0 \leq \omega < 2\pi, \quad 0 \leq \chi \leq \pi.$$

All the physical quantities depend on $k^{(a)}$ or $k^{\hat{a}}$ which in turn are uniquely specified by l and q . As discussed earlier (Pineault 1975), only certain combinations of l and q are allowed for given source and observer positions and all the possible values can be found without solving the geodesic equations. The geodesic equations are needed only to determine the relative azimuthal position ϕ .

4 Results

As an illustration, we present the results obtained when the observer is at $r_0 \rightarrow \infty$, $\theta_0 = 80^\circ$ and the source is at $r_s = 10m$ remembering that in geometrized units, $m = 1.477 \times 10^5 (m/m_\odot)$ cm with m the mass of the black hole. The calculations are only for the primary image of the source, as for the case considered, it is much brighter than any of the higher order images

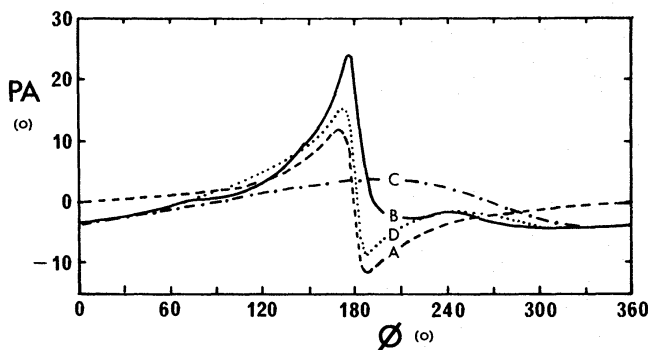


Figure 1. Position angle PA of observed radiation as a function of azimuthal position ϕ of the source. A: Source orbiting the black hole with negligible velocity ($v = 0$). B: Source orbiting the black hole with $v = v_{\text{cir}} = 0.354$. C: Source in flat space ($m \rightarrow 0$) moving with $v = v_{\text{cir}} = 0.354$. D: Sum of curves A and C. See text.

(Cunningham & Bardeen 1973; Pineault 1975) and in at least some physical situations, e.g. hot spot on accretion disk, there is likely to be absorbing material along higher-order trajectories.

In Fig. 1, we have plotted the observed position angle PA in terms of the azimuthal position ϕ of the source at the instant of emission ($\phi = 0^\circ$: source in front of the black hole; $\phi = 180^\circ$: source behind the black hole). The use of ϕ as the abscissa instead of the observed time t_0 allows direct comparison between the radiation coming from sources located at the same position on the orbit, but moving with different velocities. For a source moving with the Schwarzschild circular velocity, the orbital period is $T \approx 10^{-3}(m/m_\odot)$ s.

Several interesting features are present. First, for a source whose velocity is negligible (curve A), the position angle changes by as much as 24° over the whole orbit. Although this case does not correspond to a realistic physical situation, since the source's velocity is expected to be of the order of the circular velocity, it shows a purely general relativistic (GR) effect. As expected from geometrical considerations, the curve is antisymmetric with respect to $\phi = 180^\circ$.

When the motion of the source is taken into account (curve B) the position angle covers a somewhat larger range of $\sim 27^\circ$ and there is no obvious symmetry. This results from the standard special relativistic (SR) aberration.

The SR and GR effects can be somewhat disentangled by plotting the curve corresponding to a source in flat space ($m \rightarrow 0$, curve C) constrained to move in a circular orbit with the same velocity $v = v_{\text{cir}} = 0.354$. This exhibits the purely SR effect, whereas curve A

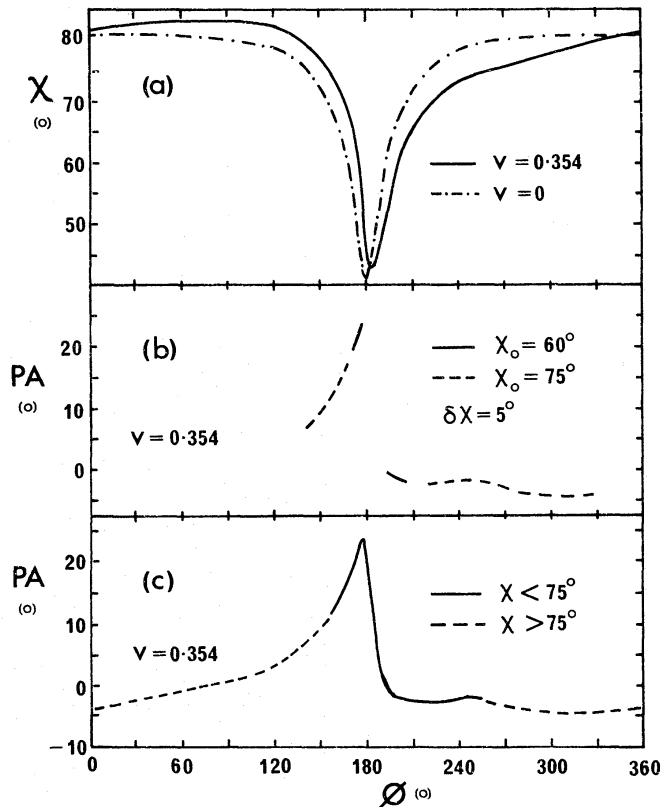


Figure 2. (a) Emission angle χ as a function of azimuthal position ϕ of the source for $v = v_{\text{cir}} = 0.354$ and $v = 0$. (b) Observed position angle PA as a function of ϕ , corresponding to a source emitting radiation only in the range $\chi = \chi_0 \pm \delta\chi$ and moving with $v = v_{\text{cir}} = 0.354$. (c) Observed PA as a function of ϕ , corresponding to radiation reaching the observer only if $\chi < \chi_{\text{max}} = 75^\circ$ (solid line). The source is moving with $v = v_{\text{cir}} = 0.354$. For comparison purposes, the dashed line shows the complementary part of the curve which is not observed.

shows the purely GR effect. Although it is clear that the two effects do not add up linearly, it is interesting to add up these two separate contributions and find that the resulting curve D broadly reproduces the general features exhibited by the original plot (curve B).

If the source emits radiation only within certain directions, for instance in a cone at polar angle χ_0 and width $\delta\chi$ (pulsar-like object) or if the radiation which is emitted at $\chi > \chi_{\max}$ is absorbed (e.g. hot spot on an accretion disk which thickens outwards), it is clear that the source will only be visible to the observer for a certain range of values of ϕ , and correspondingly only at certain times. This is shown in Fig. 2, where the polar angle of emission in the source's frame, χ , and the observed position angle PA are plotted in terms of the source's position ϕ , for a few illustrative configurations. For a given ϕ , the source can radiate to the observer only if the value of χ lies within the beaming angle $\chi = \chi_0 \pm \delta\chi$ or $\chi < \chi_{\max}$. For simplicity we have assumed the symmetry axis of the source to coincide with the z axis. The general result is that, depending on the conditions of emission, the observer will see bursts of varying duration with discontinuous jumps in the position angle.

We recall that, in view of the remarks made at the beginning of Section 2, the results presented here apply equally well to sources of arbitrary (but constant) intrinsic properties, in the sense that, although the observed position angle at a given source position depends on the given properties, the relative changes along the orbit are the same. The intensity of the radiation is of course modulated by gravitational focusing and gravitational and Doppler shifts (see, e.g. Cunningham & Bardeen 1973).

5 Discussion

Although the results presented here describe only one source—observer configuration, it appears that a discrete orbiting source with intrinsic polarization properties will exhibit significant changes in the observed position angle over an orbital period, whether the source is moving relativistically or is slowly moving in a strong gravitational field or both. If a beaming mechanism is present, discontinuous jumps in the polarization will occur. For a black hole of $10^8 m_\odot$ and the parameters used in Section 4, the orbital period is ~ 1 day, during which time the position angle changes by as much as $\sim 27^\circ$.

It will be of interest to see how strongly the effects described here depend on the distance of the source from the black hole and the observer's polar angle. If the black hole is rotating, rotation of the polarization plane will occur along a given ray and this will produce additional changes in the observed position angle. A more detailed analysis of these problems, in the context of point sources, will be presented elsewhere.

For an extended source, such as an accretion disk, more detailed calculations are needed since the resulting polarization can be described in terms of the sum of the luminosity-weighted contributions from a series of concentric rings of different radii (Lightman & Shapiro 1976). In any case the effect is likely to be frequency-dependent, as the radiation at various frequencies is predominantly emitted at different radii. This problem is presently under investigation (Richard Stark, work in progress at the University of Oxford).

Acknowledgments

The hospitality of the Institute of Astronomy, University of Cambridge, and the financial support of the National Research Council of Canada are gratefully acknowledged.

References

- Bardeen, J. M., Press, W. H. & Teukolsky, S. A., 1972. *Astrophys. J.*, **178**, 347.
Cunningham, C. T. & Bardeen, J. M., 1973. *Astrophys. J.*, **183**, 237.
Lightman, A. P. & Shapiro, S. L., 1976. *Astrophys. J.*, **203**, 701.
Pineault, S., 1975. *PhD thesis*, University of Toronto.
Pineault, S. & Roeder, R. C., 1977a. *Astrophys. J.*, **212**, 541.
Pineault, S. & Roeder, R. C., 1977b. *Astrophys. J.*, **213**, in press.
Rees, M. J., 1975. *Mon. Not. R. astr. Soc.*, **171**, 457.